Electronic Supplementary Information (ESI)

Incomplete charge transfer bestows significant sintering resistance for metal nanoparticles on two-dimensional graphyne

Min Gan,‡[a] Jiawei Huang,‡[a] Xiaodong Li,[b] Meiping Li,[b] Zhouyang Zhang,[c] Ze Yang,[d] Chunfang Zhang,[e] Peng Yang,[a] Xianglai Gan,[a] Chang Lu,[f] Xingcai Yang,[g] Linfeng Fei*[a] and Changshui Huang*[b]*

[a] School of Physics and Materials Science, Nanchang University, Nanchang 330031, China

[b] Beijing National Laboratory for Molecular Sciences, Organic Solids Laboratory, Institute of Chemistry, Chinese Academy of Sciences, Beijing 100190, China

[c] School of Materials and New Energy, Ningxia University, Yinchuan 750021, China

[d] College of Energy Storage Technology, Shandong University of Science and Technology, Qingdao 266000, China

[e] College of Chemistry and Materials Science, Hebei University, Baoding 071002, China

[f] Gatan Inc., and AMETEK Commercial Enterprise (Shanghai) Co., LTD., Pilot Free Trade Zone, Shanghai 200131, China

[g] School of Chemistry and Materials Science, Guizhou Normal University, Guiyang 550001, China

*E-mail: ncugxl@ncu.edu.cn (X. G.); feilinfeng@gmail (L. F.); huangcs@iccas.ac.cn (C. H.)

‡M. G. and J. H. contributed equally to this work.

Table of Contents

This PDF file includes:

Other Supplementary Materials for this manuscript include:

Video S1. Top-view and side-view structural evolutions of Pd NPs on HsGY and graphene upon annealing from MD simulations.

Figures and Tables

Table S1. The size of graphene and HsGY flakes used in MD simulations.

Flakes	x (Å)	y (Å)	Atom number
Graphene	239.910	241.767	21120
HsGY	240.828	241.494	7524

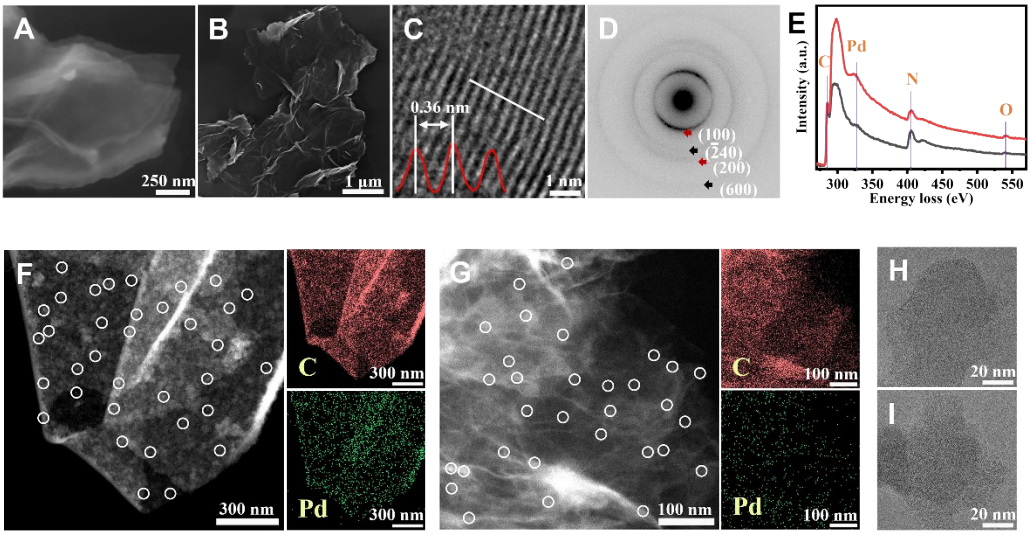

Figure S1. Microscopic characterizations of Pd NPs supported on 2D HsGY and graphene. (A, B) SEM images of HsGY and graphene-supported Pd NPs, respectively. (C) HRTEM image of HsGY with the insert showing intensity profile of HsGY lattice planes along the white line. (D) SAED pattern for the Pd NPs supported on HsGY, which simultaneously shows the diffraction rings for HsGY (black arrows) and Pd NPs (red arrows). (E) Comparison of EELS spectra for Pd/HsGY and Pd/graphene nanocatalysts. (F) HAADF-STEM image of Pd NPs on HsGY and the corresponding EDS elemental mappings for C and Pd, showing the homogenous distribution of Pd NPs on HsGY. White circles indicate a few Pd NPs. (G) HAADF-STEM image of graphene-supported Pd NPs and the corresponding EDS elemental mappings of C and Pd. White circles indicate a few Pd NPs. (H, I) Bright-field TEM images for HsGY-supported Pt and Au

samples, respectively.

HsGY and graphene flakes were used as supports to load metal NPs for in situ TEM experiments (see **Experimental section**; the atomic ratio of metal to C is controlled as ~1% across all samples). The scanning electron microscopy (SEM) images show that HsGY (**Figure S1A**) and graphene (**Figure S1B**) are both typical two-dimensional flakes with their lateral dimensions up to several microns. As shown in **Figure S1C**, the high-resolution TEM (HRTEM) image along the edge side of HsGY reveals that its interplanar distance is 0.36 nm, which is in well consistent with previous reports.[1] For HsGY flakes with Pd nanoparticles, the selected area electron diffraction (SAED) pattern (**Figure S1D**) shows clear diffraction rings from both HsGY (indicated by black arrows) and Pd (marked by red arrows) contents, as well as their good crystallinity. We then used electron energy loss spectroscopy (EELS) to compare the electronic structure of HsGY and graphene in both samples (**Figure S1E**). The high-angle annular dark-field scanning transmission electron microscopy (HAADF-STEM) images (**Figures S1F & G**) and the associated energy dispersive spectrometer (EDS) elemental mappings for C and Pd exhibits the homogenous distributions of Pd NPs (selectively marked by white circles) on both HsGY and graphene supports. In addition, other metal NPs (Pt, Au) supported on HsGY were also characterized; as shown in **Figures S1H & I**, the bright-field TEM images shows that HsGY is indeed an ideal support for distributing these noble metal NPs as nanocatalysts.

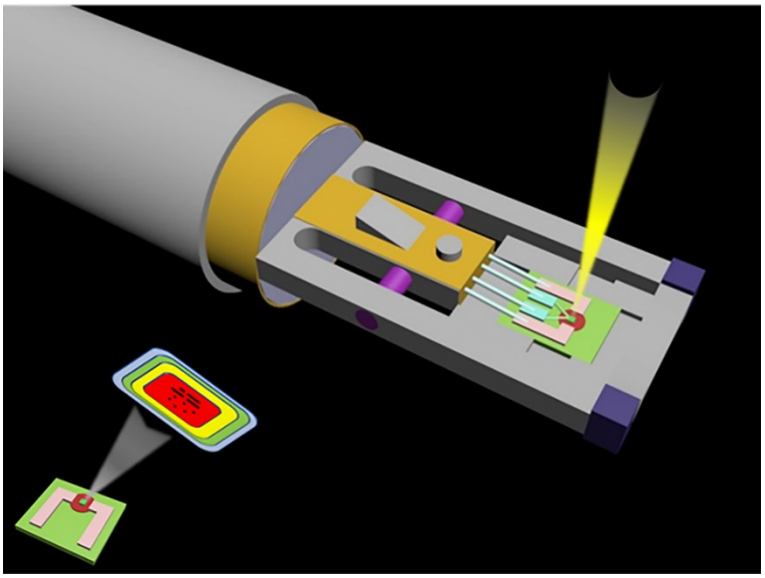

Figure S2. Schematic illustration of the setup for in situ heating TEM experiment.

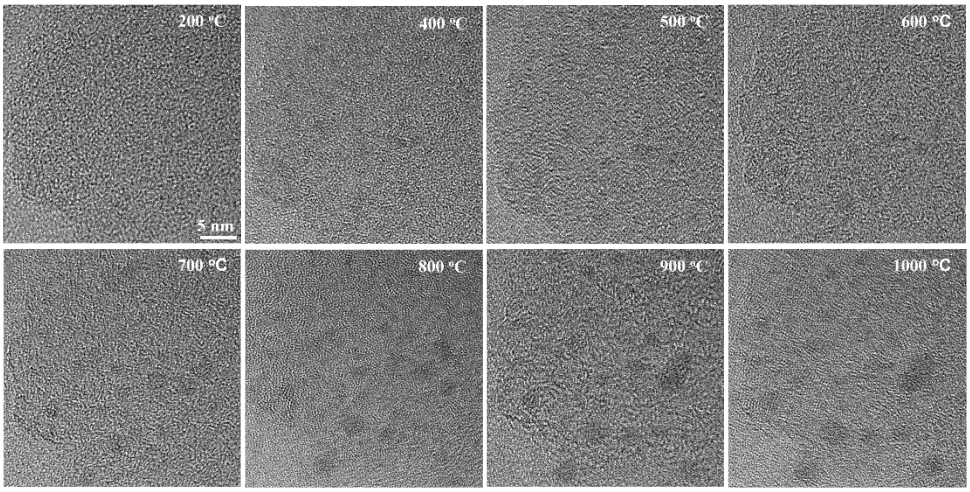

Figure S3. HRTEM image sequence showing the structural evolution of Pd NPs on HsGY support during in situ heating.

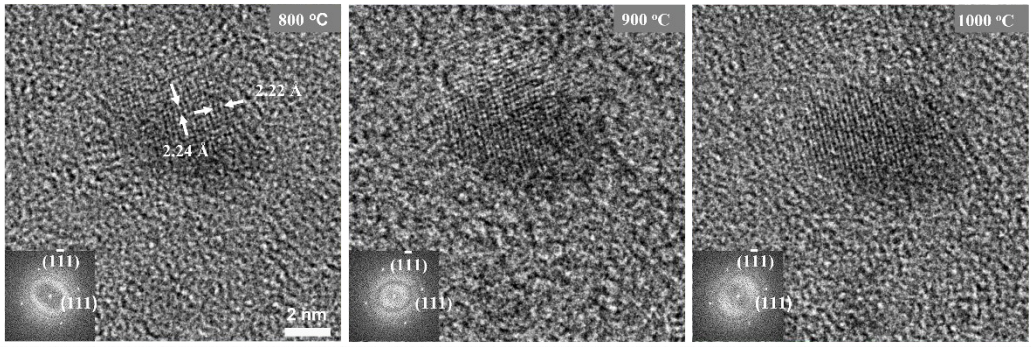

Figure S4. Lattice-resolved in situ HRTEM images for Pd NPs on HsGY annealed at different temperatures. Insets are the corresponding FFT patterns for NPs.

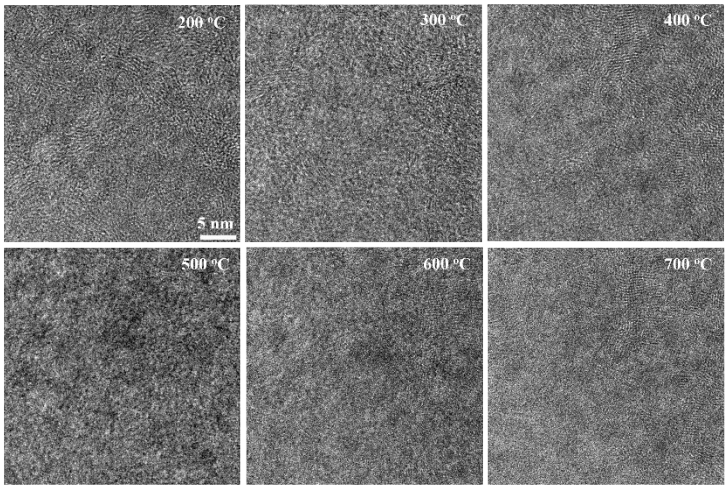

Figure S5. TEM images for structural evolution of Pd NPs on graphene support during in situ heating.

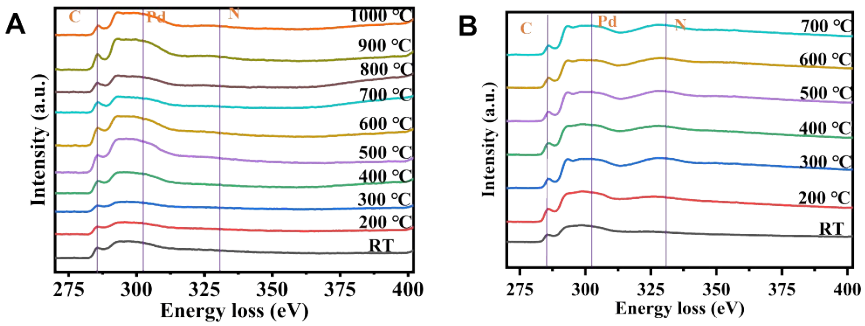

Figure S6. Temperature-dependent EELS spectra during in situ annealing of Pd supported on (A) HsGY and (B) graphene supports.

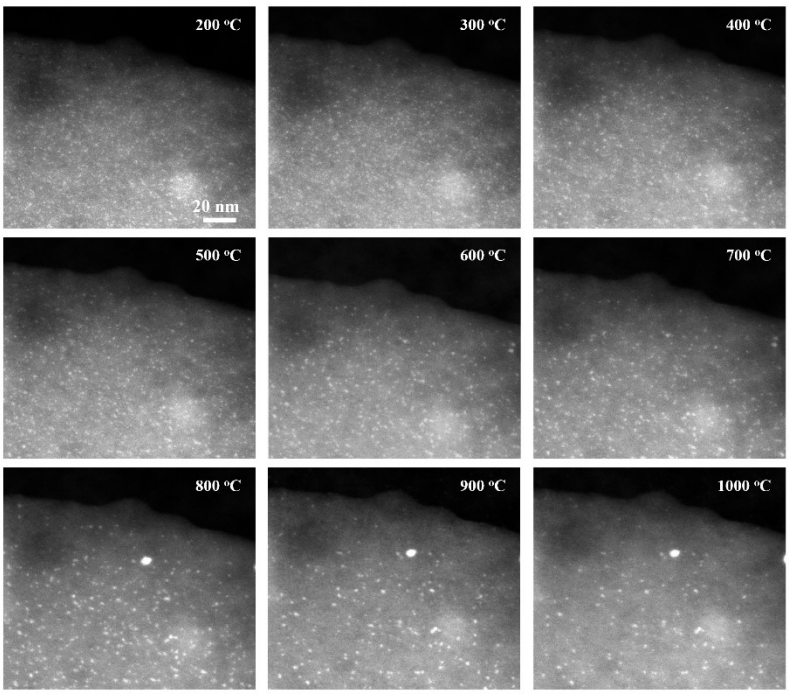

Figure S7. STEM image sequence showing the thermal stability of Pd NPs on HsGY support during in situ heating.

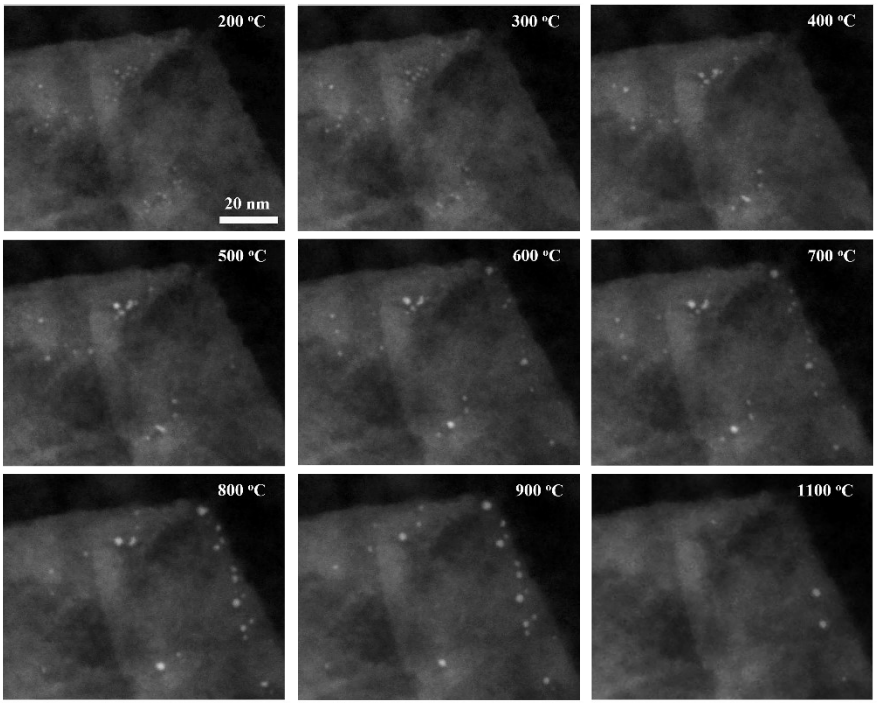

Figure S8. STEM image sequence showing the thermal instability of Pd NPs on graphene support during in situ heating.

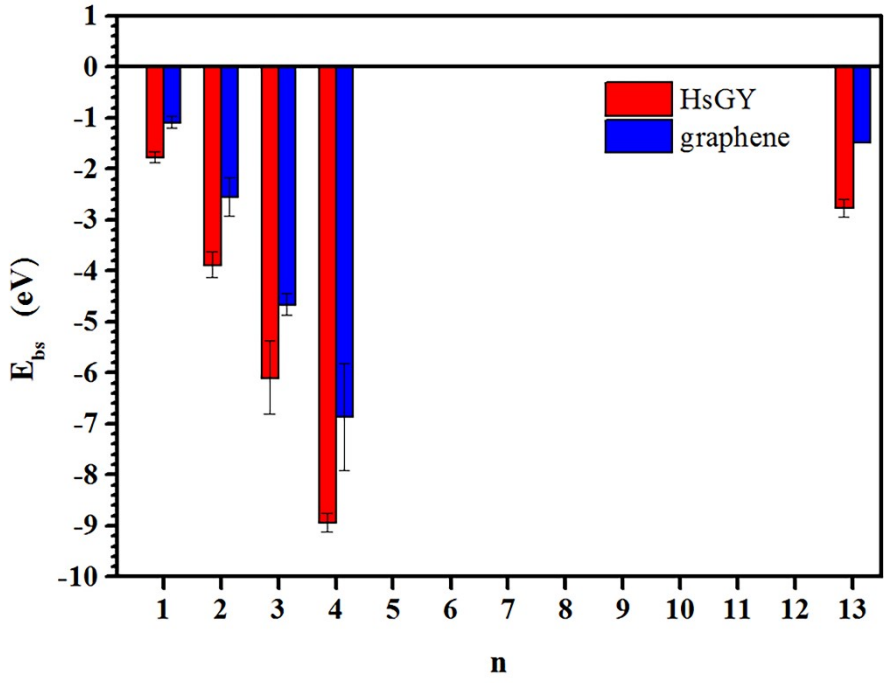

Figure S9. Average E_{bs} for one, two, three, four Pd atoms and Pd_{13} cluster absorbed at different sites of HsGY and graphene.

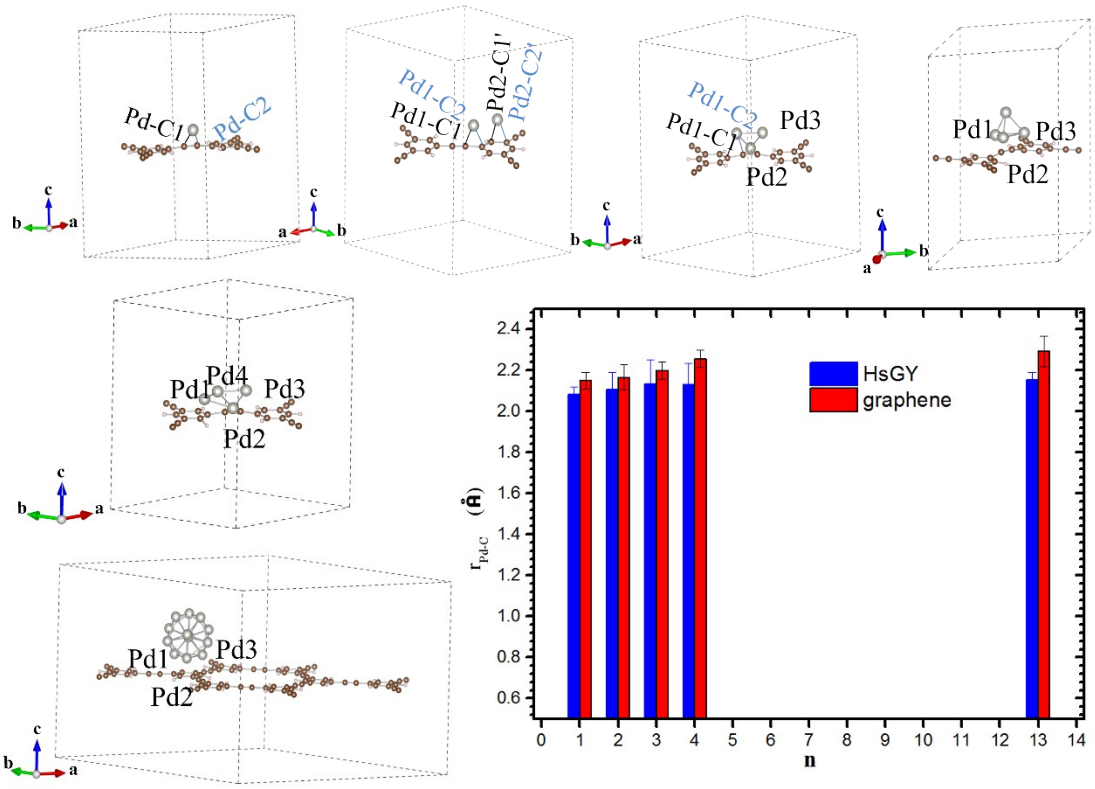

Figure S10. Average atomic distances between the Pd atoms and the nearest carbon atoms of the interface.

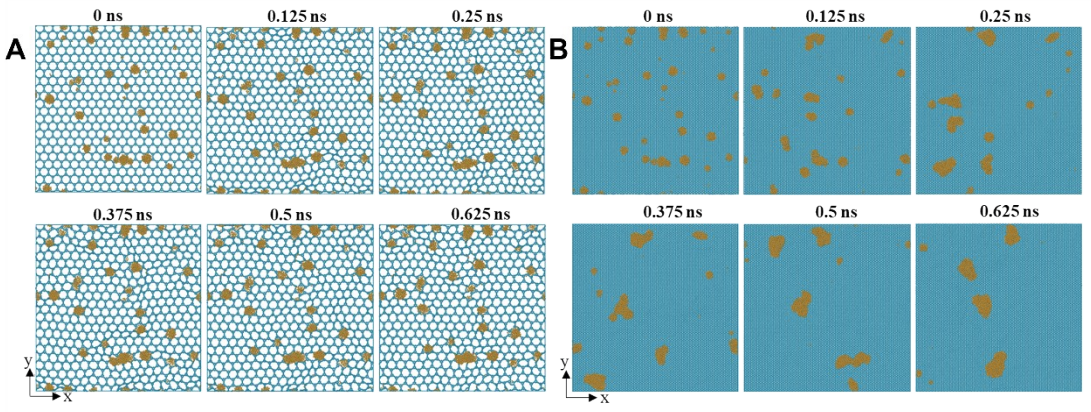

Figure S11. Microstructural evolutions for sintering of Pd NPs on HsGY and graphene supports by MD simulations. Top-view images of structural evolution as a function of annealing time for (A) Pd/HsGY and (B) Pd/graphene systems.

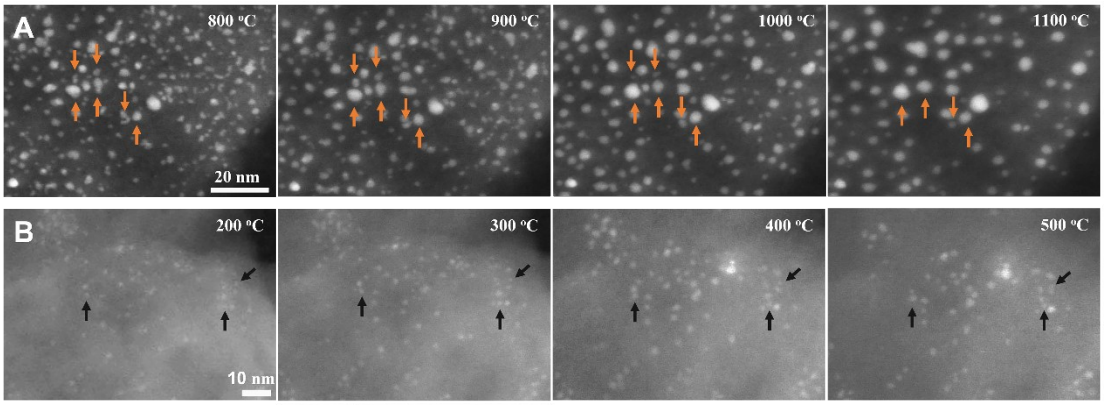

Figure S12. **HADDF-STEM images for the sintering mechanisms of HsGY and graphene-supported Pd NPs.** (A) HADDF-STEM images of the OR process (indicated by orange arrows) for HsGY-supported Pd NPs. (B) HADDF-STEM images of the PMC processes of Pd NPs on graphene support (indicated by black arrows).

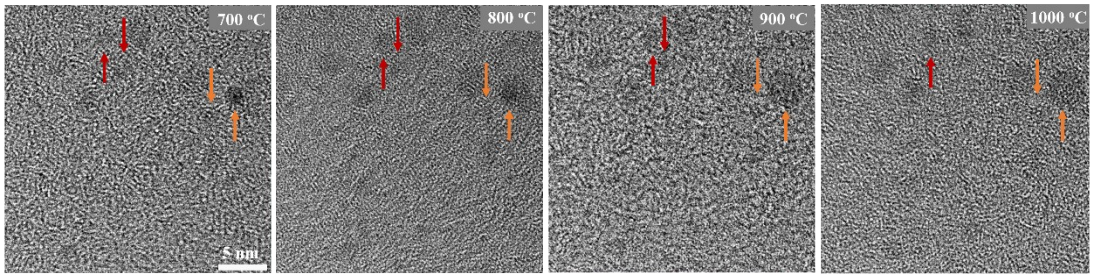

Figure S13. HRTEM images for the OR process of HsGY-supported Pd NPs. The orange and red arrows showing the growth and shrinkage of Pd NPs.

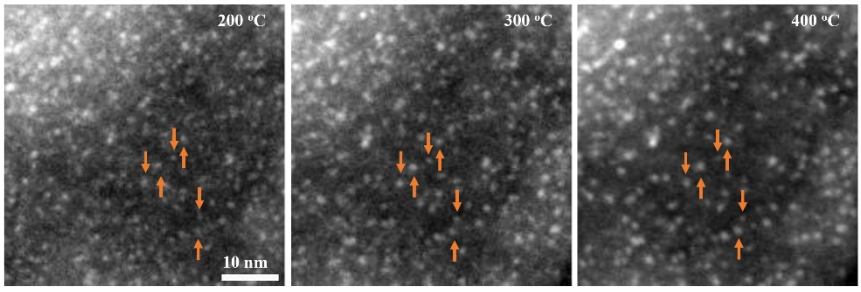

Figure S14. HADDF-STEM images for the OR process of HsGY-supported Pd NPs.

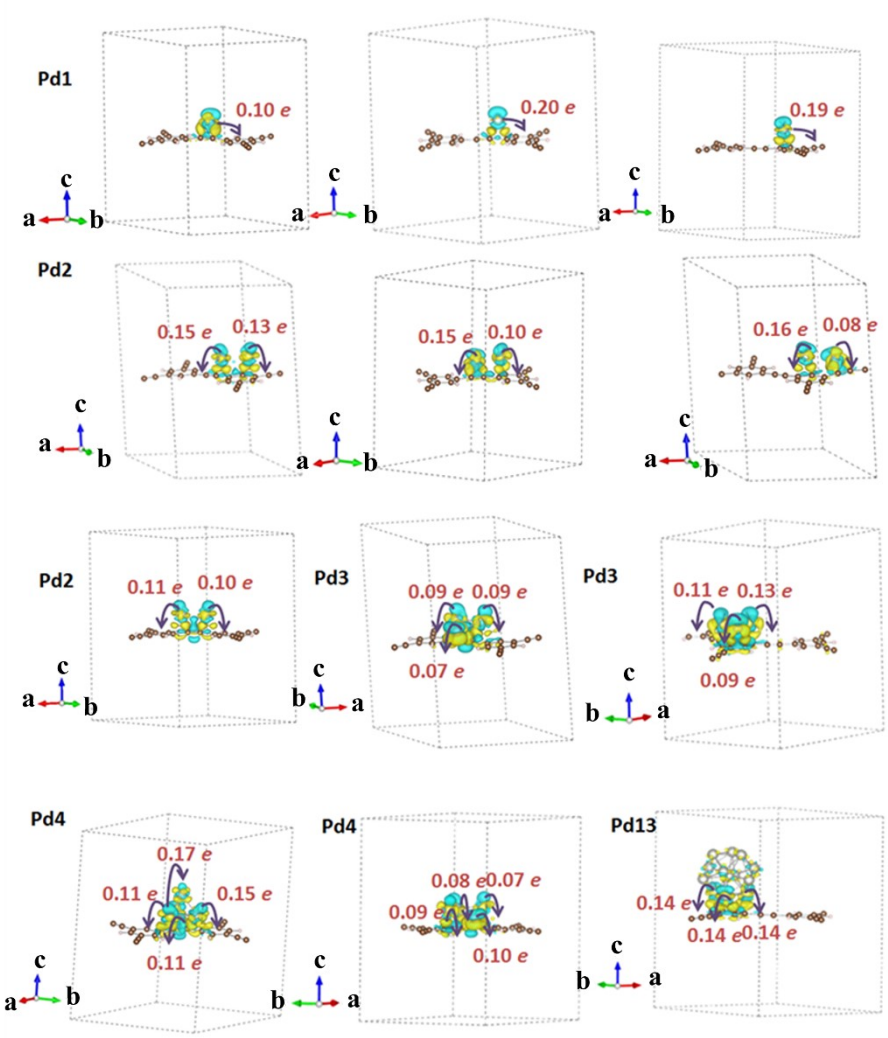

Figure S15. Bader charge of each Pd atoms on HsGY. Yellow color means charge accumulation and green shows the depletion of charge.

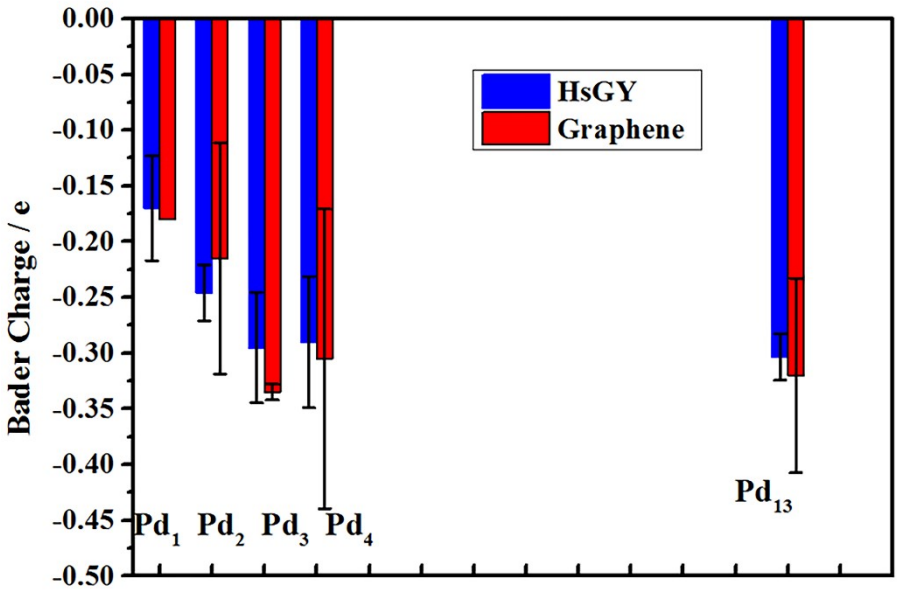

Figure S16. Average Bader charges transferred from specific Pd particles to the HsGY or graphene support.

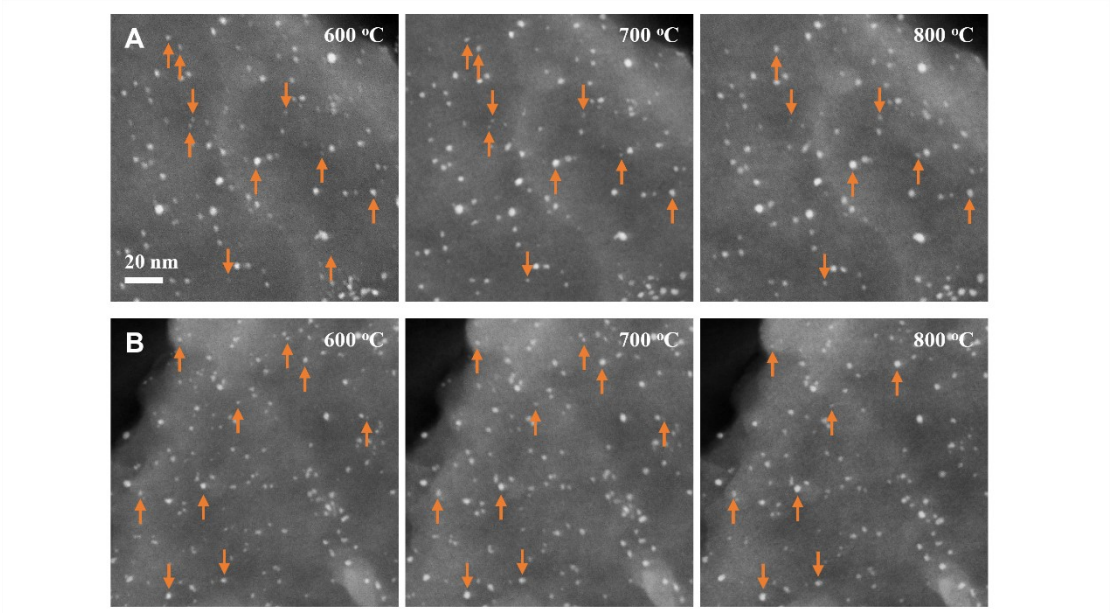

Figure S17. STEM images of the OR process for HsGY-supported Pt and Au NPs, respectively. (A) OR for HsGY-supported Au NPs. (B) OR for HsGY-supported Pt NPs. The orange arrows showing the growth and shrinkage of metal NPs. The scale bar in the first panel of (A) applies to all the others.

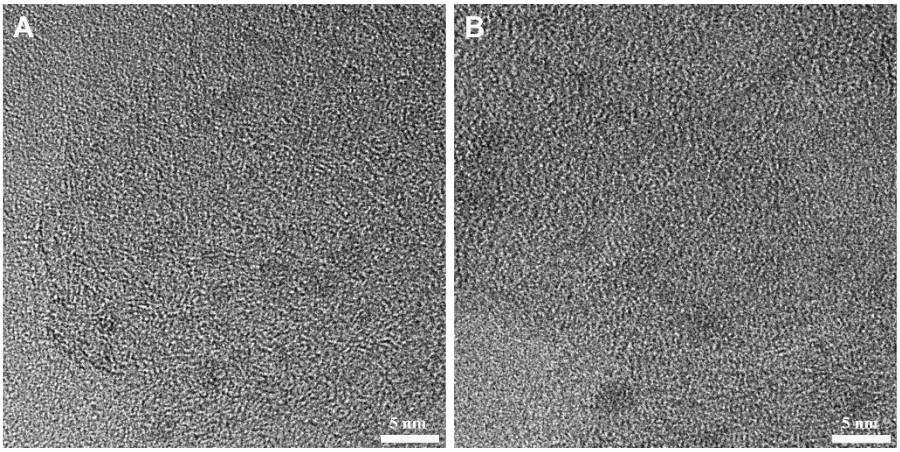

Figure S18. Effect of electron beam irradiation on Pd NPs supported by HsGY. (A) TEM image of an irradiated region during an in situ experiment. (B) TEM image of an unirradiated region far from the position of (A) during the in situ experiment.

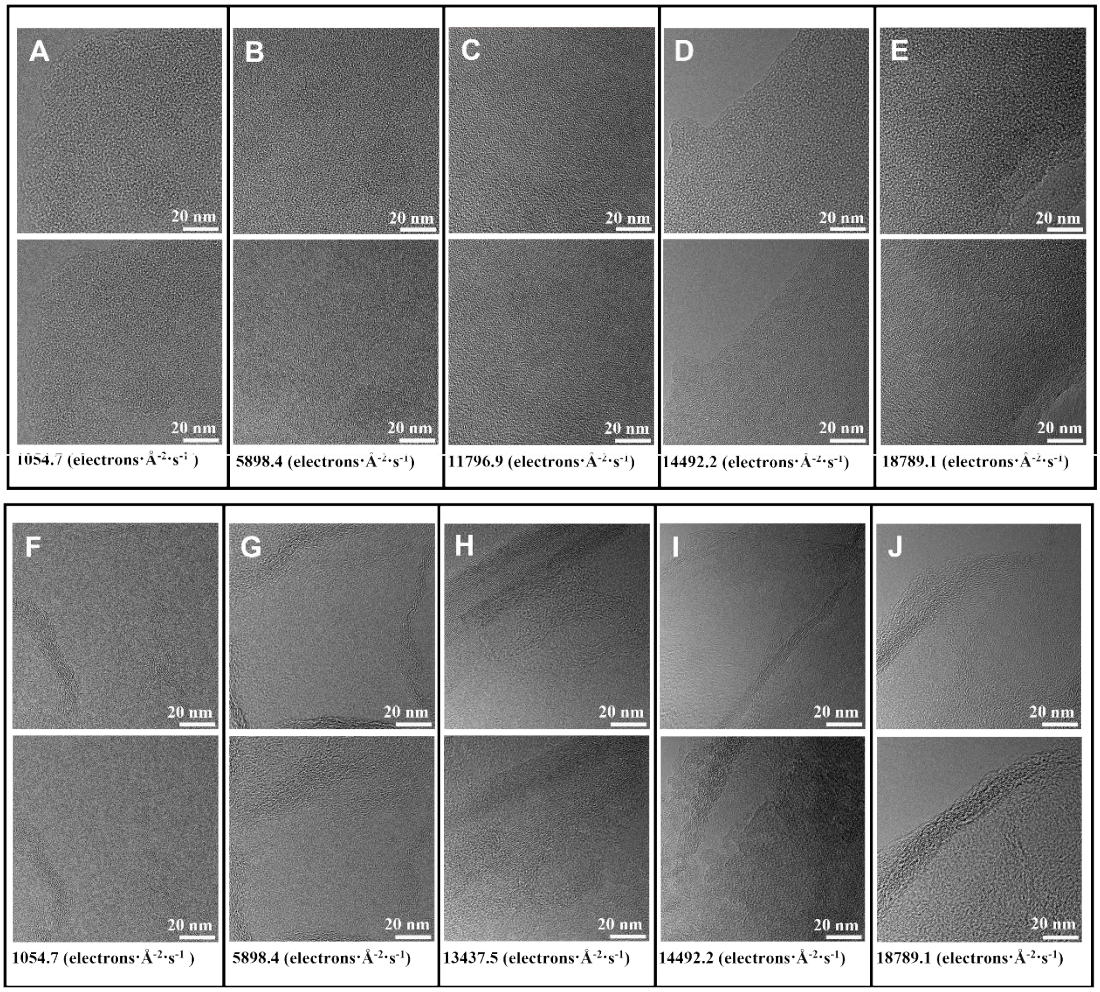

Figure S19. Effect of electron beam density on Pd NPs supported on HsGY and graphene. (A-E) TEM image comparison of HsGY-supported Pd NPs upon irradiation with different densities for 15 minutes. The beam density for (A), (B), (C), (D), and (E) is 1054.7, 5898.4, 11796.9, 14492.2, and 18789.1 electrons·Å^{-2}·s^{-1}, respectively. (F-J) TEM image comparison of graphene-supported Pd NPs upon irradiation with different densities for 15 minutes. The beam density for (F), (G), (H), (I), and (J) is 1054.7, 5898.4, 13437.5, 14492.2, and 18789.1 electrons·Å^{-2}·s^{-1}, respectively.

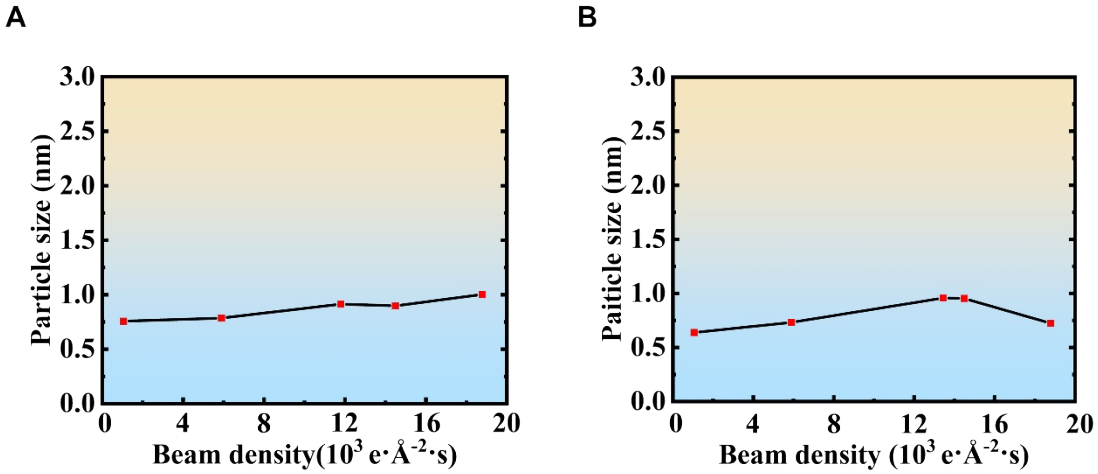

Figure S20. Plot of beam density versus particle size after 15 minutes of electron beam irradiation. (A) Influence of electron beam intensity on the size of HsGY-supported Pd NPs. (B) Influence of electron beam intensity on the size of graphene-supported Pd NPs.

In situ TEM experiments are often suffered from the complex sample-electron interactions.[2] In order to exclude the possible effect of electron beam on particle size of metal NPs during prolonged irradiation (it should be noted that most of our experiment were performed under STEM mode, in which the irradiation effect is very small), a series of control experiments were also performed. Firstly, a simple comparison in **Figure S18** shows the HRTEM images between a region which was continuously irradiated by electron beam during in situ heating and another region which was far away from the beam; the Pd NPs across the two images basically have similar size and size distributions, undoubtedly suggesting the neglectable effect of electron beam on particle size in our experiment.[3] Secondly, systematical evaluation of the beam density on Pd NPs supported on HsGY/graphene was further carried out; TEM images of HsGY/graphene-supported Pd NPs irradiated with different electron beam density for 15 minutes are shown in **Figure S19**, and the corresponding plot on particle size versus beam density is shown in **Figure S20**. These results, again, quantitatively confirms that the as-observed particle sintering behaviors are mostly resulted from the heating process.

References

1 Z. Yang, C. Zhang, Z. Hou, X. Wang, J. He, X. Li, Y. Song, N. Wang, K. Wang, H. Wang and C. Huang, *J. Mater. Chem. A*, 2019, **7**, 11186-11194.

2 Q. Chen, C. Dwyer, G. Sheng, C. Zhu, X. Li, C. Zheng and Y. Zhu, *Adv. Mater.*, 2020, **32**, 1907619.

3 L. Fei, S. M. Ng, W. Lu, M. Xu, L. Shu, W.-B. Zhang, Z. Yong, T. Sun, C. H. Lam, C. W. Leung, C. L. Mak and Y. Wang, *Nano Lett.*, 2016, **16**, 7875-7881.